

Small Fermi energy and phonon anharmonicity in MgB_2 and related compounds

L. Boeri¹, G.B. Bachelet^{1,2}, E. Cappelluti¹, L. Pietronero^{1,2,3}

¹*INFM Unità di Roma 1 and Dipartimento di Fisica,
Università di Roma "La Sapienza", P.le Aldo Moro 2, 00185 Roma, Italia*

²*INFM Center for Statistical Mechanics and Complexity, P.le Aldo Moro 2, 00185 Roma, Italia and*

³*CNR, Istituto di Acustica "O.M. Corbino", v. del Fosso del Cavaliere 100, 00133 Roma, Italy*

(Dated: October 30, 2018)

The remarkable anharmonicity of the E_{2g} phonon in MgB_2 has been suggested in literature to play a primary role in its superconducting pairing. We investigate, by means of LDA calculations, the microscopic origin of such an anharmonicity in MgB_2 , AlB_2 , and in heavily hole-doped graphite. We find that the anharmonic character of the E_{2g} phonon is essentially driven by the small Fermi energy of the σ holes. We present a simple analytic model which allows us to understand in microscopic terms the role of the small Fermi energy and of the electronic structure. The relation between anharmonicity and nonadiabaticity is pointed out and discussed in relation to various materials.

PACS numbers: 74.70.Ad, 63.20.Ry, 63.20.Kr

The report of superconductivity at $T_c = 39$ K in MgB_2 [1] has raised great expectations about metal diborides MB_2 . There is indeed no reason to believe that MgB_2 represents the highest- T_c compound within this family. Since the very beginning a generic consensus about the electron-phonon (e-ph) nature of the superconducting pairing has prevailed [2, 3], although some purely electronic models have been proposed [4]. The precise origin of such a high- T_c superconducting phase is still unknown. Recently the strong anharmonic character of the in-plane E_{2g} phonon mode and its possible correlation with the high T_c value in MgB_2 have attracted a considerable interest [5, 6, 7, 8, 9]. Here we attempt a simple theory of such a strong anharmonicity and test its predictive power on related compounds. With this perspective we have performed first-principles calculations of the band structure and lattice properties of MgB_2 , AlB_2 , and of a hypothetical hole-doped graphite. We identify the small value of the Fermi energy for the holes in the σ band, with entire portions of the Fermi surface disappearing upon E_{2g} distortion [7, 10], as the fundamental origin of anharmonicity; a simple way of modeling the effect of distortion on the band structure confirms our finding. It has already been pointed out in literature that MgB_2 resembles in many ways graphite [2, 11, 12, 13]. From the structural point of view MgB_2 is formed by graphene-like layers of B spaced by planes of Mg atoms. The point group symmetry of in-plane boron phonon modes of MgB_2 and in-plane phonons of graphite is thus the same [6], and the difference in frequency is related to the different strength of B-B and C-C bonds. Out of the whole vibrational spectrum, a large interest has converged towards the E_{2g} mode in MgB_2 , which involves only in-plane boron displacements. This mode has been shown to have an extremely strong coupling with the in-plane σ bands [2, 3, 5, 6, 7, 8, 9], which in MgB_2 provide conduction holes; a relation to the high superconducting temperature T_c was naturally suggested. This idea

was also supported by the negligible partial isotope coefficient on T_c associated with the Mg atomic mass [14]. In this context the strong anharmonicity, a unique property of the E_{2g} phonon within the MgB_2 vibrational spectrum [5, 6], acquires an obvious importance. The electronic structure of MgB_2 shares strong similarities with graphite. In both materials one can identify strongly two-dimensional σ bands, almost entirely derived from B (C) s and $p_{x,y}$ orbitals, plus bonding and antibonding π bands with three-dimensional dispersion and mainly B_{p_z} -Mg (C_{p_z}) character. The most important difference between MgB_2 and graphite is the position of the Fermi level μ . In undoped graphite μ cuts the π band structure just in the middle, about 3 eV above $\epsilon_{\sigma}^{\text{top}}$, the top of the bonding σ bands, which are thus completely full [15]. In MgB_2 the combined effect of additional magnesium layers, different ionic charge between boron and carbon, and valence-charge transfer from magnesium to boron layers, yields a different arrangement of σ and π bands. The resulting Fermi level μ still cuts the π band structure somewhere, but is now ~ 0.5 eV below the top of the σ bands, which therefore, in MgB_2 , give a sizable hole contribution to the Fermi surface [11, 13], not present in graphite. This important difference was almost immediately pointed out [13]; more recently the large splitting and shifts which the σ bands undergo upon typical E_{2g} phonon displacements were suggested as the likely source of anharmonicity for the E_{2g} phonon in MgB_2 [5]. We are going to make this statement more precise. We claim that neither the presence at the Fermi level of the σ bands nor their strong coupling to the E_{2g} phonon are sufficient to induce anharmonic effects: it's the small Fermi energy associated, in the unperturbed crystal, to the σ conduction holes ($\epsilon_{\sigma}^{\text{top}} - \mu \simeq 0.45$ eV) which makes the difference. On these grounds we may expect anharmonic effects to be strong in other materials with small Fermi energies (and sufficient e-ph coupling), and also conjecture a relation between anharmonic and nonadiabatic ef-

fects. We present local Density Functional [16] calculations, based on Martins-Troullier pseudopotentials [17] and the ABINIT code [18], which support this picture; the resulting bands and E_{2g} frozen-phonon energies are well understood in terms of a simple model, discussed in the second part of this letter. We studied the E_{2g} phonon for MgB_2 , AlB_2 , graphite and a hypothetical hole-doped graphite where one electron is missing from each carbon atom. Experimental lattice parameters were used as an input for MgB_2 , AlB_2 and graphite, while for hole-doped graphite the lattice parameters were left at the experimental value of graphite. For the purpose of this study the use of GGA's and an extremely accurate *a priori* determination of equilibrium lattice parameters are not an issue. Great care in the \mathbf{k} -space integration is, instead, an issue [6], since, in some cases, entire portions of the Fermi surface disappear upon distortion; we use two $15 \times 15 \times 10$ shifted Monkhorst-Pack grids in the Brillouin zone [18]. We should also specify that, between the two possible eigenvectors for the E_{2g} phonon, we only show results for the one labeled $E_{2g}(b)$ in Ref.[6], whose energy is, by symmetry, an even function of the displacement; phonon displacements up to $0.05 \sim 0.1 \text{ \AA}$ were considered. The first important observation is that the E_{2g} anharmonicity is completely absent in AlB_2 , whose σ bands undergo equally large splittings and shifts as MgB_2 . As shown in Fig. 1, our frozen- E_{2g} -phonon calculations reproduce the large anharmonicity found for MgB_2 (black squares) [5, 6], but predict no such effect for AlB_2 (empty squares), whose energy remains proportional to the square of the phonon displacement for all the displacements under consideration. Our finding is consistent with the experimental fact that the E_{2g} phonon line is very broad in MgB_2 but not in AlB_2 [3].

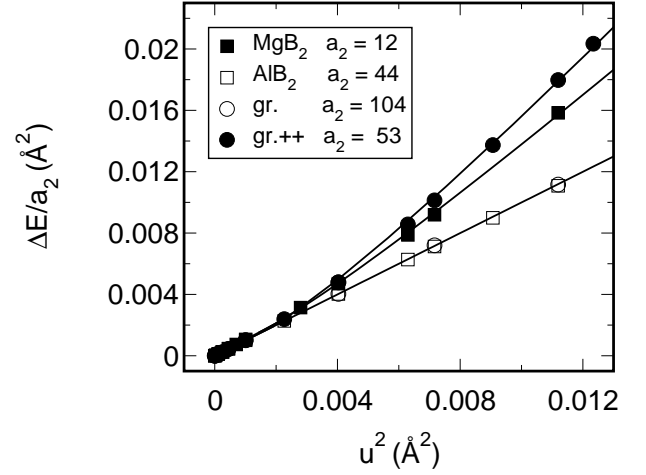


FIG. 1: Energy ΔE associated to an E_{2g} phonon displacement of amplitude u , plotted as a function of u^2 . For each material this energy is divided by a_2 (in the inset, units of $\text{eV}/\text{\AA}^2$), the quadratic coefficient of a polynomial best fit $\Delta E \simeq a_2 u^2 + a_4 u^4 + \dots$. On both axes the units are thus \AA^2 , and harmonic phonons collapse on a single straight line $y = x$. The solid lines result from our model (Eqs. 3 and 5); the corresponding parameters are shown in Table I.

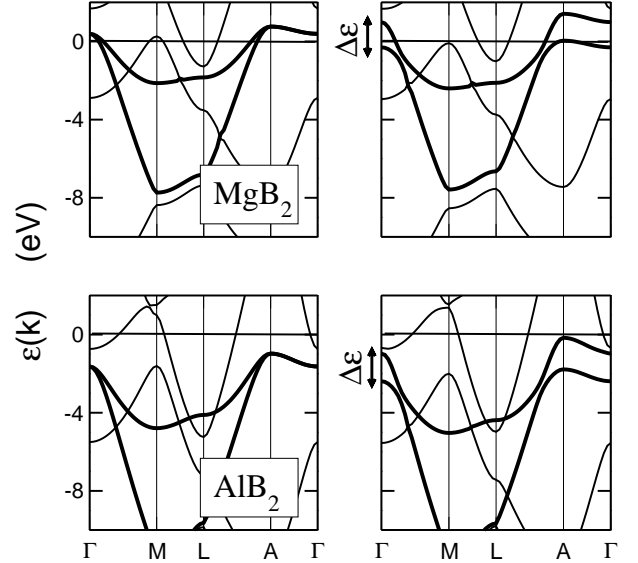


FIG. 2: Upper panels: MgB_2 electronic bands without (left) and with (right) an E_{2g} phonon distortion of amplitude $u = 0.05 \text{ \AA}$. Lower panels: same as upper panels, but for AlB_2 and $u = 0.05 \times (a_{\text{AlB}_2}/a_{\text{MgB}_2}) \text{ \AA}$. The σ bands are marked as thicker lines. Their splitting upon E_{2g} distortion is equally large in MgB_2 and AlB_2 , but in the latter (lower panels) they are always below the Fermi level ($\mu = 0$ in all panels).

We suggest that the different behavior of AlB_2 be simply related to the fact that, both before and after the E_{2g} distortion, its σ bands are near, but completely below, the Fermi level μ ; unlike MgB_2 , their electronic occupation remains unchanged upon distortion (see Fig. 2). In MgB_2 , instead, the top of the σ bands is above the Fermi

energy but, upon distortion, the lower splitoff band completely sinks below it, thus changing its occupation. Besides the amount of the shifts and splittings, the exact position of the σ bands before and after the E_{2g} distortion is thus a crucial ingredient for its anharmonicity. This is confirmed by artificially moving the top of these bands, ϵ_{σ}^{top} , w.r.t. the Fermi level μ in graphite. In true graphite the σ bands also undergo large splittings, but they are already well below μ both before and after the E_{2g} distortion; here our frozen- E_{2g} -phonon calculations find no anharmonicity (Fig. 1, empty dots; “gr.” stays for graphite). But if, by adding a uniform neutralizing background [13], we remove one electron per carbon atom (two electrons per cell, black dots in Fig. 1) from graphite, thus shifting ϵ_{σ}^{top} , the top of its σ bands, back to the “optimal” position (~ 1 eV above μ in the undistorted crystal), then, upon typical E_{2g} distortions, the lower splitoff σ band sinks below μ , and we recover strong anharmonic effects, shown in Fig. 1 (black dots). To clarify the origin of this anharmonic behavior we have traced back the effect of the E_{2g} frozen-phonon distortion to the electronic structure. For all materials we find that the main effect of the lattice displacement is a linear energy splitting of the σ bands. The π bands are,

	g	ϵ_{σ}^{top}	a ₂
MgB ₂	12.02	0.45	12
AlB ₂	11.74	-1.63	44
gr.	28.29	-2.89	104
gr.++	30.86	1.17	53

TABLE I: Three inputs for our total energy model, Eqs. (3) and (5), extracted from our LDA outputs. The remaining two parameters N_{σ} and N_{π} , needed only when $\epsilon_{\sigma}^{top} > \mu$, were adjusted to yield the best fits shown in Fig. 1. Their optimal values ($N_{\sigma} = 0.11$, $N_{\pi} = 0.39$ for MgB₂; $N_{\sigma} = 0.07$, $N_{\pi} = 0.30$ for graphite++) fall in a physically reasonable range, in spite of our oversimplified density of states (see text).

instead, only weakly modified. The effects of lattice distortion on the band structure, in a relevant energy range around the Fermi level μ , can be thus schematized, to a good approximation, as $\delta\epsilon_{\sigma}(\mathbf{k}) \simeq \pm g|u|$, with opposite signs for the two different σ bands. The value of g deduced from the LDA results differs significantly between the borides (MgB₂, AlB₂) and graphite (with or without doping), while it is almost constant within each class of compounds (see Table I). From the comparison of the band structures in Fig. 2 we can identify two representative cases. For AlB₂ (bottom) the bonding σ bands, at zero distortion (left), are completely below the Fermi level μ , and remain there upon distortion (right); their energy splitting, induced by the E_{2g} lattice displacement, does not change either their occupation or the topology of the Fermi surface, which never acquires a σ sheet; no σ band crosses μ at any displacement, and the Fermi surface is exclusively dictated by the π bands, which, compared to the σ bands, undergo only minor changes

upon displacement. Besides AlB₂, this is also the case of undoped graphite (not shown). An entirely different situation is found when, on one hand, the top of the bonding σ bands at zero distortion, ϵ_{σ}^{top} , is above the Fermi level μ (so that in the perfect crystal the Fermi surface has σ -hole-like cylindrical sheets [11]), but, on the other, the energy splitting of the σ bands is large enough to drive one of them completely below μ upon distortion. This is the case of MgB₂ (top Fig. 2), and also of heavily hole-doped graphite (not shown). In both cases, at some critical phonon displacement, the number of Fermi surfaces associated to the σ bands changes (one of the two cylindrical sheets around the Γ -A line disappears [7]); beyond that point, since the total number of electrons is conserved, larger displacements will imply a qualitatively different behavior, due to the reshuffling of electrons between σ and π states. To gain further insight, we present a simple model of the E_{2g} anharmonicity which seems to represent well both types of situations. We first consider the system with no distortion ($u = 0$). The electronic band energy can be written as:

$$E(u=0) = 2 \sum_{\mathbf{k}, i} \epsilon_i(\mathbf{k}) n_i(\mathbf{k}) + 2 \sum_{\mathbf{k}} \epsilon_{\pi}(\mathbf{k}) n_{\pi}(\mathbf{k}), \quad (1)$$

where $\epsilon_i(\mathbf{k})$ represents the dispersion relation of the two σ bands, $\epsilon_{\pi}(\mathbf{k})$ takes into account the remaining π bands, and $n_i(\mathbf{k})$, $n_{\pi}(\mathbf{k})$ are the corresponding occupations (the factor 2 is for the spin degeneracy). The LDA bands teach us that the most important effect of an E_{2g} distortion $u \neq 0$ is an almost linear splitting (i.e. proportional to u) of the two σ bands around the Γ -A line. This can be roughly modeled by a linear e-ph Jahn-Teller-like coupling of the E_{2g} phonon to the σ bands; the small coupling to the π bands is neglected altogether. The resulting total energy at $u \neq 0$ is:

$$E(u) = 2 \sum_{\mathbf{k}, i} \epsilon_i(\mathbf{k}) n_i(\mathbf{k}, u) + 2 \sum_{\mathbf{k}} \epsilon_{\pi}(\mathbf{k}) n_{\pi}(\mathbf{k}, u) + 2gu \sum_{\mathbf{k}} [n_2(\mathbf{k}, u) - n_1(\mathbf{k}, u)] + \frac{M\omega_{2g}^2}{2} u^2 \quad (2)$$

In Eq. (2) the electronic band energy, in the presence of a phonon displacement u , was split into the sum of three terms: unperturbed σ and π bands with u -dependent occupation (first two terms in the r.h.s), plus a linear e-ph coupling of the E_{2g} mode with the σ bands. The last term is an effective elastic energy. Far from the Fermi level our bands are not realistic (see below), so we lump into this term both the bare ion-ion repulsion and those electronic effects which are missing from our model bands. The occupation number can be self-consistently calculated: $n_1(\mathbf{k}, u) = f[\epsilon_1(\mathbf{k}) - gu - \mu(u)]$, $n_2(\mathbf{k}, u) = f[\epsilon_2(\mathbf{k}) + gu - \mu(u)]$, $n_{\pi}(\mathbf{k}, u) = f[\epsilon_{\pi}(\mathbf{k}) - \mu(u)]$, where $\mu(u)$ is the Fermi level in the presence of the frozen phonon and $f[x] = \theta(-x)$ is the $T=0$ Fermi function.

Let us consider the representative case of MgB_2 . For the sake of simplicity we assume two parabolic σ bands, perfectly two-dimensional and degenerate at $u = 0$ [$\epsilon_1(\mathbf{k}) = \epsilon_2(\mathbf{k}) = \epsilon_\sigma(\mathbf{k})$]. The corresponding density of states (DOS) of each σ band will be therefore constant up the top of the band $\epsilon_\sigma^{\text{top}}$: $N_\sigma(\epsilon) = N_\sigma$ [$\epsilon \leq \epsilon_\sigma^{\text{top}}$]. From now on we conveniently set $\mu(u=0) = 0$, so that $\epsilon_\sigma^{\text{top}}$ now equals $\epsilon_\sigma^{\text{top}} - \mu(u=0)$, the Fermi energy of the σ holes in the absence of lattice distortion. In addition, in the energy range we are interested of, we can assume N_π , the density of states of the π band, to be just constant. The Fermi level $\mu(u)$ and the total energy $E(u)$ in the presence of the frozen phonon distortion u can now be easily computed. The system shows a qualitatively different behavior for two interesting regimes: (i) $g|u| \leq \epsilon_\sigma^{\text{top}}$ and (ii) $g|u| \geq \epsilon_\sigma^{\text{top}}$. Within the assumptions of our model (rectangular DOS), in the regime (i) the Fermi level is unaffected by the frozen phonon distortion, $\mu(u) = \mu(u=0) = 0$: the depletion of the σ band, raised by the distortion, is compensated by an equivalent filling of the other σ band, lowered by the same amount; the π bands, modeled by their constant DOS N_π , play no role. We obtain for the total energy:

$$E(u) = E(0) + \frac{M\omega_{2g}^2}{2}u^2 - 2N_\sigma g^2 u^2 \quad g|u| \leq \epsilon_\sigma^{\text{top}}. \quad (3)$$

Eq. (3) represents a phonon frequency renormalization due to the response of the σ electrons, $E(u) = E(0) + M\Omega_{2g}^2 u^2/2$, with $\Omega_{2g}^2 = \omega_{2g}^2 - 4N_\sigma g^2/M$. The harmonic character of the E_{2g} phonon mode is however unaffected. Things change in the regime (ii) $g|u| \geq \epsilon_\sigma^{\text{top}}$. When the energy splitting is larger than the zero-distortion Fermi energy of the σ holes, $g|u| \leq \epsilon_\sigma^{\text{top}}$, the lower σ band is completely shifted below the Fermi level. Now this band is full, and cannot further compensate the loss of electrons from the upper σ band. Then the only way to conserve their total number is to add more electrons to the π bands, which thus come into play. To obtain this, the Fermi level needs to shift, and the dependence on u of the total energy, is, in turn, deeply modified:

$$\mu(u) = \frac{N_\sigma}{N_\sigma + N_\pi} (g|u| - \epsilon_\sigma^{\text{top}}) \quad g|u| \geq \epsilon_\sigma^{\text{top}}. \quad (4)$$

$$E(u) = E(0) + \frac{M\omega_{2g}^2}{2}u^2 - 2N_\sigma g^2 u^2 + \frac{N_\sigma(2N_\sigma + N_\pi)}{N_\sigma + N_\pi} (g|u| - \epsilon_\sigma^{\text{top}})^2 \quad g|u| \geq \epsilon_\sigma^{\text{top}}. \quad (5)$$

In our simple model the transition between harmonic and anharmonic regime occurs when one band is completely shifted below the Fermi level, and does not manifest itself as a simple additional quartic term u^4 . Rather, an overall anharmonic potential results from a simple harmonic term up to $g|u| \leq \epsilon_\sigma^{\text{top}}$ which, for $g|u| \geq \epsilon_\sigma^{\text{top}}$, smoothly connects to a shifted parabola with different curvature.

Such a non-analytic behaviour has to do with the extreme simplifications of our model, in particular with the perfectly 2D parabolic character of the σ bands (step-like density of states), and on the assumption of perfect degeneracy of the σ bands at $u = 0$ [$\epsilon_1(\mathbf{k}) = \epsilon_2(\mathbf{k})$]. We have checked that, with slightly more realistic models, the sharp transition of Eq. (5) becomes considerably smoother. However, Eq. (5) is particularly appealing just because of its simplicity, since it depends only on a few parameters which can be extracted from LDA calculations (see Table I), thus providing a direct test of the model. The results are shown as solid lines in Fig. 1 for the compounds considered here. The agreement with LDA first-principles calculations is quite good, considering the extreme simplifications of our model. In conclusion, in this paper we have investigated, by means of numerical and analytical techniques, the microscopic nature of the anharmonicity of the E_{2g} phonon mode in MgB_2 . The results presented here provide a clear evidence that the anharmonicity of the E_{2g} phonon mode in MgB_2 is induced by the extremely small value of the σ -hole Fermi energy. Along this view we can predict a strong anharmonicity in heavily hole-doped graphite. We have shown that the anharmonicity of the E_{2g} mode, which is strongly coupled to the σ bands, can be considered a signature of small Fermi energy; this points out in a natural way towards the possibility of nonadiabatic effects. A quantitative description of this situation involves, however, quantum-many-body effects (nonadiabatic renormalization of the phonon frequencies[19]). While this task is beyond the aim of the present paper, different theoretical studies already suggest that nonadiabatic effects could be responsible for the high T_c in MgB_2 [20, 21]. Note that this is entirely different from the initial claim [5], that anharmonicity affects superconductivity via the nonlinear coupling. From this point of view the situation is, instead, similar to fullerenes [22], which have been recently shown to reach critical temperatures as high as $T_c = 117\text{K}$ in FET doped compounds [23]. In this respect our work suggests new perspectives in the search for high- T_c materials. In particular, heavily hole-doped graphite, which we predict to have small Fermi energy and anharmonic E_{2g} phonon, would be a potential candidate for high- T_c superconductivity. The recent claim of $T_c = 35\text{K}$ in amorphous graphite-sulfur composite samples could be related to this scenario [24].

-
- [1] J. Nagamatsu, N. Nakagawa, T. Muranaka, Y. Zenitani, J. Akimitsu, Nature **410**, 63 (2001).
 - [2] Y. Kong, O.V. Dolgov, O. Jepsen, and O.K. Andersen, Phys. Rev. B **64**, 020501 (2001).
 - [3] K.-P. Bohnen, R. Heid, and B. Renker, Phys. Rev. Lett. **86**, 5771 (2001).
 - [4] J.E. Hirsch, Phys. Lett. A **282**, 392 (2001).

- [5] T. Yildirim, O. Gulseren, J.F. Lynn, C.M. Brown, T.J. Udovic, Q. Huang, N. Rogado, . A. Regan, M.A. Hayward, J.S. Slusky, T. He, M.K. Haas, P. Khalifah, K. Inumaru, and R.J. Cava, Phys. Rev. Lett. **87**, 037001 (2001).
- [6] K. Kunc, I. Loa, K. Syassen, R.K. Kremer, K. Ahn, J. Phys.: Cond. Mat. **13**, 9945 (2001).
- [7] A.Y. Liu, I.I. Mazin, and J. Kortus, Phys. Rev. Lett. **87**, 087005 (2001).
- [8] H. J. Choi, D. Roundy, H. Sun, M. L. Cohen, S. G. Louie, cond-mat/0111182 (2001).
- [9] V.V. Struzhkin, A.F. Goncharov, R.J. Hemley, H. K. Mao, G. Lapertot, S. L. Bud'ko, P. C. Canfield, cond-mat/0106576 (2001).
- [10] This is quite different from what discussed in K.P. Meletov, J. Arvanitidis, M.P. Kulakov, N.N. Kolesnikov, G.A. Kourouklis, cond-mat/0110511 (2001), where a σ -band splitting was assumed even in the undistorted lattice.
- [11] J. Kortus, I.I. Mazin, K.D. Belashchenko, V.P. Antropov, L.L. Boyer, Phys. Rev. Lett. **86**, 4656 (2001).
- [12] G. Satta, G. Profeta, F. Bernardini, A. Continenza, S. Massidda, Phys. Rev. B **64**, 104507 (2001).
- [13] J.M. An, W.E. Pickett, Phys. Rev. Lett. **86**, 4366 (2001).
- [14] D.G. Hinks, H. Claus, J.D. Jorgensen, Nature **411**, 457 (2001).
- [15] M.S. Dresselhaus and G. Dresselhaus, Adv. Phys. **30**, 139 (1981).
- [16] P. Hohenberg e W. Kohn, Phys. Rev. **136**, B864 (1964); W. Kohn e L.J. Sham, Phys. Rev. **140**, A1133 (1965).
- [17] N. Troullier, J. L. Martins, Phys. Rev. B **43**, 1993 (1991).
- [18] The ABINIT code is a common project of the Université Catholique de Louvain, Corning Incorporated, and other contributors (URL <http://www.abinit.org>).
- [19] A.S. Alexandrov and H. Capellmann, Phys. Rev. B **43**, 2042 (1991).
- [20] A.S. Alexandrov, Physica C **363**, 231 (2001).
- [21] E. Cappelluti, S. Ciuchi, C. Grimaldi, L. Pietronero, and S. Strässler Phys. Rev. Lett. **88**, 117003 (2002).
- [22] E. Cappelluti, C. Grimaldi, L. Pietronero, and S. Strässler, Phys. Rev. Lett. **85**, 4771 (2000).
- [23] J.H. Schön, Ch. Kloc, and B. Batlogg, Science **293**, 2432 (2001).
- [24] R. Ricardo da Silva, J. H. S. Torres, and Y. Kopelevich, Phys. Rev. Lett. **87**, 147001 (2001).